Textile & Leather Review

ISSN 2623-6281| www.tlr-journal.com | 10.31881/TLR

Emotional Response Mechanism of Smart Textiles Integrated with Transformer Model in Garden Interactive Art Installation

Tianlong Chai, Chengcheng Sha

How to cite: Chai T, Sha C. Emotional Response Mechanism of Smart Textiles Integrated with Transformer Model in Garden Interactive Art Installation. Textile & Leather Review. 2026; 9:80-99. https://doi.org/10.31881/TLR.2026.080

How to link: https://doi.org/10.31881/TLR.2026.080

Published: 20 January 2026

Emotional Response Mechanism of Smart Textiles Integrated with Transformer Model in Garden Interactive Art Installation

Tianlong CHAI[1], Chengcheng SHA[2*]

[1]College of Civil and Architecture engineering, Guangxi University of Science and Technology, Liuzhou 545006, Guangxi, China

[2]Department of Economics and Trade, Guangxi Eco-Engineering Vocational & Technical College, Liuzhou 545004, Guangxi, China
*shacheng1995@126.com

Article
https://doi.org/10.31881/TLR.2026.080
Received 30 July 2025; Accepted 27 October 2025; Published 20 January 2026

ABSTRACT

To address the challenge that smart textiles face in achieving multimodal emotion perception and personalized artistic responses in complex garden environments, this paper proposes an emotion recognition and artistic feedback mechanism based on a lightweight Transformer model. By integrating electromyography (EMG), galvanic skin response (GSR), and voice sensors within smart textiles, users' physiological signals and environmental data are collected, and multi-source information is fused to extract emotional characteristics. Combined with a metaphorical emotion-art mapping strategy, the light-emitting diode (LED) array and shape memory materials in the textiles are driven to generate dynamic color and morphological changes. This mechanism is applied to interactive garden art installations that integrate natural elements such as plants and terrain, with the generated artistic feedback synergistically responding to the natural environment. The model is optimized through a lightweight design, enabling real-time deployment. Experimental results show that the system achieves an average EMG signal-to-noise ratio (SNR) of 28.3 dB in interactive garden art installations and compresses the response delay to 190 ms in complex garden scenes. User satisfaction surveys indicate that the scores for joy and calmness emotional feedback are 4.25 and 4.05, respectively. This paper provides a feasible technical path for the application of smart textiles in the field of emotional interaction and art installations.

KEYWORDS
smart textiles, interactive garden art installations, transformer model, emotion perception, multimodal data fusion

INTRODUCTION

The application of smart textiles in the field of interactive art has attracted widespread attention in recent years. Their ability to realize environmental perception and dynamic response by integrating sensors and actuators provides a new form of expression for art installations [1,2]. In the interactive art scene of gardens, interactive devices need to operate under complex conditions such as open spaces, dynamic lighting, temperature and humidity fluctuations, and vegetation interference, taking into account the dynamic changes of the natural environment and the personalized recognition of user emotions. Traditional systems mostly rely on a single sensor or static feedback mechanism, making it difficult to capture the complexity and real-time nature of emotions [3]. Existing technologies face many challenges: there is a semantic gap in multimodal physiological and environmental data, which leads to inaccurate extraction of emotional features; complex models are difficult to run efficiently on resource-constrained textile embedded platforms; and the mapping between emotional states and artistic expressions lacks a dynamic association mechanism, limiting interactive immersion and the effectiveness of emotional transmission [4,5].

The application of smart textiles in emotion recognition and regulation has garnered widespread attention, with research focusing on integrating multimodal interaction mechanisms and physiological signal monitoring technologies. Xiaowei Chen et al. proposed the ASSURE model framework to analyze the regulatory mechanisms of sensory stimulation and immersion on emotional experience [6]. This perspective further promoted Mengqi Jiang's exploration of smart textiles based on motion interaction [7]. His research integrated emotion regulation strategies into interactive design to enhance the intervention effect of physical participation on emotional state. Bekinew Kitaw Dejene approached the issue from a physiological monitoring perspective [8]. By reviewing the application of wearable textiles in emotion management, he verified the feasibility of combining sensor technology with psychological principles and multimodal feedback to enhance users' self-awareness. Mengqi Jiang et al. [9] systematically sorted 75 emotionally interactive textiles and further refined the research boundaries. The seven functional goals and feedback forms they summarized clarified the correlation between the interaction mechanism and the function of textiles. Mengqi Jiang and other researchers developed a prototype of smart clothing called E-motionWear, which integrates motion detection sensors with three feedback mechanisms: audio, visual, and vibrotactile [10]. The prototype explores the impact of body movement-based interactions on emotion regulation. However, existing research still faces the contradiction between the complexity of emotion recognition models and the limited resources of embedded platforms, the difficulty of semantic alignment in multimodal data fusion, and the lack of systematic construction of dynamic mapping mechanisms between emotional states and artistic feedback.

The application of deep learning technology has improved the capabilities of smart textiles in multimodal emotion recognition and real-time response. Ngoc-Dau Mai et al. combined an improved visual Transformer with an ear electroencephalogram (EEG) to optimize remote emotion monitoring [11]. Saurabh Kumar used LSTM (Long Short-Term Memory), GRU (Gated Recurrent Unit), and CNN (Convolutional Neural Network) to enhance the accuracy of cross-modal emotion recognition [12]. With the popularity of wearable devices, Sihem Nita et al. proposed a convolutional neural network method based on data augmentation for emotion recognition from electrocardiogram (ECG) signals [13]. Yujin Wu et al. designed a self-supervised framework to alleviate the problem of data scarcity [14]. Felicia Andayani et al. proposed a hybrid model that combines an LSTM network with a Transformer encoder for speech emotion recognition [15]. This model uses Melfrequency cepstral coefficients (MFCCs) to extract speech features and combines the LSTM's ability to model temporal dependencies with the Transformer's global attention mechanism to effectively capture long-term dependencies in speech. However, existing deep models still face challenges: the large amount of computation makes it difficult to adapt to resource-constrained textile embedded platforms; the cross-modal feature alignment mechanism lacks dynamic adjustment capabilities and is unable to cope with data heterogeneity and dynamic changes caused by light, temperature, humidity, and user activities in the garden environment; and the self-supervised framework mostly relies on predefined tasks and does not combine the real-time interactive characteristics of textiles to optimize lightweight training strategies.

To address the emotional response problem of smart textiles in interactive garden art installations, this study proposes an emotional response framework based on a lightweight Transformer model. The hardware layer integrates electromyography, electrodermal activity, and voice sensors to build a multimodal data acquisition system and designs low-noise preprocessing to eliminate environmental interference. The algorithm layer adopts the Mobile Transformer architecture and uses its cross-modal attention mechanism to dynamically model the semantic associations between heterogeneous data sources, overcoming noise interference in the garden environment. It combines local attention to optimize computing efficiency and compresses model parameters through knowledge distillation to adapt to embedded real-time reasoning. The interaction layer analyzes the intensity of emotions based on attention weights, drives the LED array and shape memory materials in the textiles to generate dynamic artistic feedback, and establishes a nonlinear mapping between emotional features and artistic expressions. This method applies the contextual modeling capability of the Transformer model to smart textiles, breaks through performance bottlenecks through lightweight design and cross-modal fusion, and provides a scalable technical path for emotion-driven environmental fusion art interaction in complex garden environments.

DESIGN OF EMOTION PERCEPTION AND RESPONSE SYSTEM BASED ON LIGHTWEIGHT TRANSFORMER

System Architecture Design

To address the challenges of open environmental interference, heterogeneity in multimodal data, and the natural integration of artistic feedback in interactive garden art scenes, this study has designed a closed-loop emotional response system architecture. This architecture deeply integrates data perception, emotion recognition, dynamic mapping, and artistic feedback modules, thereby establishing a comprehensive link between user emotion perception and environmental collaborative expression. The overall architecture design is shown in Figure 1.

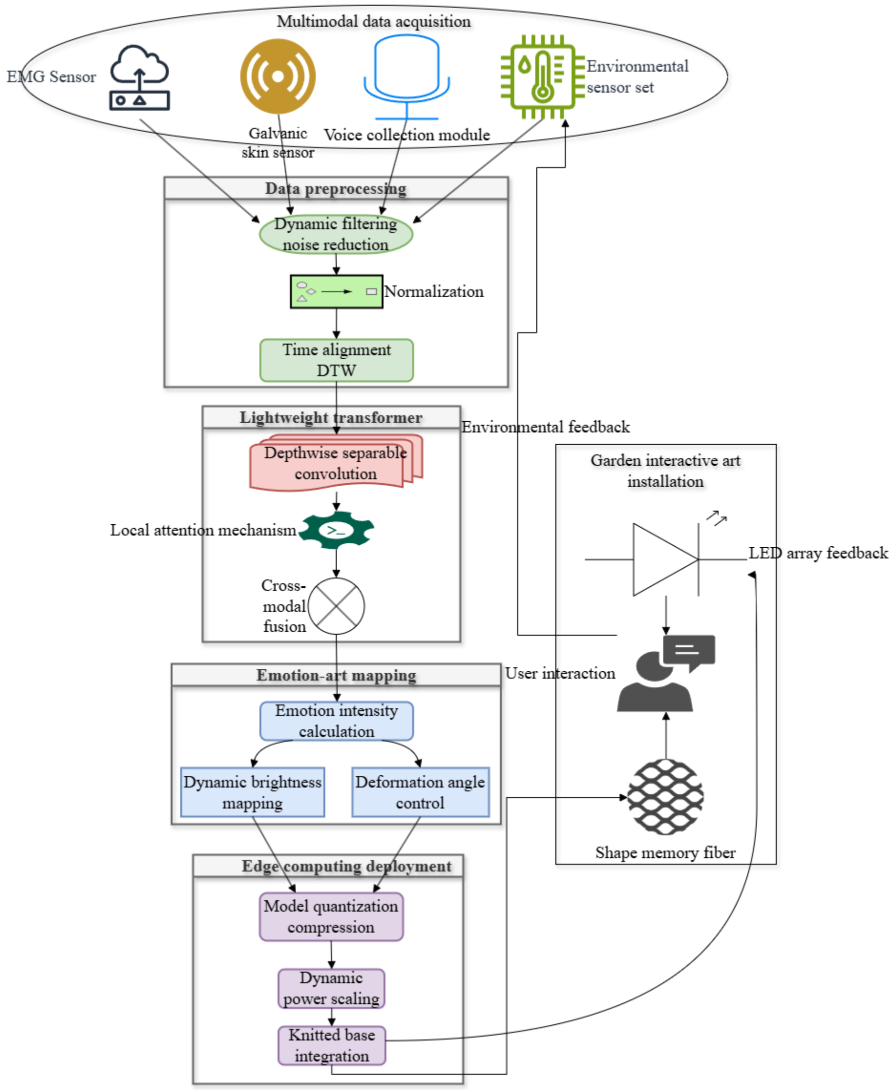

Figure 1. System architecture design

Figure 1 shows a closed-loop interactive architecture with smart textiles as the core. The multimodal data acquisition module collects user physiological signals (electromyography (EMG), EDA, voice) and simultaneously monitors key environmental variables (light intensity, temperature, humidity) that can indirectly affect emotion recognition by introducing noise into the physiological signals. For instance, high humidity can increase electrodermal activity (EDA) signal noise due to sweat, and strong light fluctuations can cause motion artifacts in EMG signals. The system uses this environmental data to dynamically filter out such noise, ensuring the purity of the input to the emotion recognition model. After dynamic filtering, denoising, normalization, and Dynamic Time Warping (DTW) alignment, the data is input into the lightweight Transformer model, and local features are extracted through deep separable convolution. The local attention mechanism and cross-modal fusion strategy are combined to generate the emotion intensity value. This value drives the emotion-art mapping module, dynamically controls the brightness gradient of the LED array and the deformation angle of the shape memory fiber, and realizes the natural artistic feedback of color and form.

After 8-bit integer quantization and dynamic voltage frequency regulation optimization, the lightweight model is deployed on an embedded platform with an integrated knitted substrate. Finally, the dynamic response of the LED array and shape memory fiber triggers user interaction, and its feedback data is re-input into the system through environmental sensors, forming a real-time emotional interaction closed loop in complex garden scenes.

Multimodal Data Acquisition and Preprocessing Module

The electromyography, galvanic skin response, and voice acquisition modules are integrated into smart textiles, with sensors embedded in the knitted structure through conductive fibers and flexible circuits. These can be used to monitor dynamic changes in lighting, temperature, and humidity in the garden environment, as well as noise changes caused by user movement [16]. Silver-coated fiber electrodes collect physiological signals, and environmental data, such as light intensity, temperature, and humidity, are acquired synchronously through a distributed micro-sensor array. The environmental sensors specifically measure light intensity (lux), ambient temperature (°C), and relative humidity (%). These data are not direct inputs for emotion recognition but are used as contextual features to filter out environmental noise and to dynamically adjust the cross-modal attention weights, ensuring the emotion recognition model remains robust in varying garden conditions. To reduce the motion artifact interference in the electromyographic signal and the potential electromagnetic interference in the garden environment, a fourth-order Butterworth bandpass filter (20–450 Hz) is applied to the EMG signal to isolate the myoelectric activity, followed by a notch filter at 50 Hz to eliminate power line interference. This filtering strategy follows established protocols in surface electromyography analysis [17]. Its transfer function is:

$$H(s)=\frac{1}{(s^2+1.414s+1)(s^2+0.765s+1)} \tag{1}$$

In formula (1), s is the Laplace variable, which is used to suppress high-frequency noise and retain the characteristic frequency band of electromyography; 1.414 and 0.765 are the damping coefficients corresponding to the first and second pairs of conjugate poles of the Butterworth low-pass filter, which ensure the maximum flat amplitude response in the passband and guarantee the overall frequency characteristics of the fourth-order filter; 1 is the normalized constant term represents the standard Butterworth filter with a cutoff frequency of 1 rad/s. To eliminate the baseline drift of the EDA (electrodermal activity) signal caused by individual differences, a high-pass filter with a cutoff frequency of 0.05 Hz is applied for baseline correction. This process separates the slow-varying tonic component from the fast phasic responses, thereby facilitating inter-subject comparability. The formula is:

$$x'=\frac{x\text{-}x_{min}}{x_{max}\text{-}x_{min}} \tag{2}$$

In formula (2), x is the original signal, x_{min} and x_{max} are the minimum and maximum values of the signal, respectively, so that the range of the processed signal is constrained to the interval [0, 1]. The speech signal suppresses common background noises such as wind, bird calls, and human voices in the garden through an adaptive filtering algorithm. A 64-tap NLMS (Normalized Least Mean Squares) filter with a step size of 0.1 is used to suppress these specific noise sources. The reference input for the NLMS filter is provided by a dedicated omnidirectional background noise microphone, which captures the ambient soundscape without the user's voice, enabling effective cancellation of wind, bird calls, and distant human voices from the primary speech signal. The weight update formula is:

$$w(n+1)=w(n)+\mu e(n)x(n) \tag{3}$$

In formula (3), μ is the step size factor; $e(n)$ is the error signal; and $x(n)$ is the input vector. The minimum mean square error criterion optimizes the filter coefficients. The multimodal data is time-aligned through the dynamic time warping algorithm, and the optimal path distance between sequence A and B is calculated:

$$D(A,B)=\sqrt{\sum_{k=1}^{K} (a_k-b_k)^2} \tag{4}$$

In formula (4), a_k and b_k are feature points obtained after timestamp matching, and K is the path length, which addresses the timing misalignment problem caused by the differing sampling frequencies of various sensors. The preprocessed data is input into the emotion recognition model through the feature extraction module, completing the conversion from the original signal to the emotion feature vector.

Lightweight Transformer Emotion Recognition Model Design

Based on the results of multimodal data preprocessing, a lightweight Transformer architecture is constructed to model emotional states. Unlike Transformer models designed for sequential text data, which rely on self-attention to capture linguistic dependencies, our model adapts the cross-modal attention mechanism to dynamically model the complex, asynchronous, and heterogeneous relationships between physiological signals (EMG, EDA, voice) and environmental dynamics (light, temperature), addressing the unique challenges of non-sequential, real-time multimodal fusion in a noisy outdoor setting. The model adopts the Mobile Transformer structure, replacing the fully connected layer in the original Transformer with depth-separable convolution. The calculation formula is:

$$Conv_{depthwise}(x)=\sum_{c=1}^{C} x_c*w_c \tag{5}$$

$$Conv_{pointwise}(x)=\sum_{c=1}^{C} Conv_{depthwise}(x_c)\cdot w_{1\times 1,c} \tag{6}$$

In formulas (5) and (6), x_c is the input feature of the C-th channel; w_c is the depth convolution kernel; and $w_{1\times1,c}$ is the point-by-point convolution kernel. The amount of calculation is reduced by decomposing the convolution operation. In the design of the attention mechanism, a local attention module is applied to limit the calculation range of the dot product of the query vector Q and the key vector K. The formula is:

$$Attention(Q,K,V)=softmax\left(\frac{QK^T}{\sqrt{d_k}}\odot M\right)V \tag{7}$$

In formula (7), d_k is the scaling factor and M is the mask matrix, which avoids redundant calculations of global attention. In the cross-modal fusion stage, the semantic alignment of EMG, EDA, and speech features is achieved through cross-modal attention, and the weight generation formula is:

$$\alpha_i=softmax\left(\mathrm{h}_i^T W_a \mathrm{h}_m\right) \tag{8}$$

In formula (8), h_i is the target modal feature; h_m is the auxiliary modal feature; W_a is the learnable parameter matrix, and the generated weight α_i is used to fuse multimodal information in a weighted manner. Knowledge distillation is used in the model compression stage, with the large Transformer as the teacher model and the lightweight model as the student model, to minimize the KL (Kullback-Leibler) divergence loss of the output probability distributions of the two:

$$\mathrm{L}_{distill}=KL\left(Softmax\left(\frac{z_t}{T}\right)\|Softmax\left(\frac{z_s}{T}\right)\right) \tag{9}$$

In formula (9), z_t and z_s are the output logits of the teacher and student models, and T is the temperature coefficient. The generalization ability of the lightweight model is improved through parameter migration. The final model is deployed on the embedded chip, and the weights are compressed from 32-bit floating points to 8-bit integers using the Qwen-Quantize toolchain.

Emotion-Artistic Feedback Mapping Strategy Construction

Based on the emotion recognition results, a dynamic art feedback mechanism is constructed, and a multimodal response is achieved through the embedded LED array and shape memory fiber in the knitted structure [18,19]. Six basic emotional states, such as joy and sadness, are defined, and a nonlinear mapping relationship between emotion intensity and artistic expression parameters is established. For instance, “joy” is mapped to a bright, warm yellow light that expands outward in a sunflower-like pattern, symbolizing vitality and openness. "Calmness" is represented by a gentle, blue wave pattern that slowly undulates. Conversely, "anger" triggers a sharp, red flash with rapid, jagged deformation, while "fear" is expressed through a flickering, dim purple light and a sudden, inward contraction. This strategy uses nature-inspired metaphors to translate abstract emotions into tangible, intuitive, and aesthetically coherent artistic feedback. The normalization of the attention weight α_i of the Transformer model generates the emotion intensity value $E\in [0, 1]$:

$$E=\frac{\sum_{i=1}^{N} \alpha_i \cdot w_i}{max(\alpha_i)} \tag{10}$$

In formula (10), w_i is the weight coefficient of the emotion feature, and N is the feature dimension. The emotion intensity value E is defined as a normalized measure of the model's confidence in the dominant emotion classification. It is derived from the attention-weighted sum of the output logits for the dominant emotion category, which is then normalized to the [0, 1] range. This value reflects the degree of activation or salience of the detected emotion, regardless of its valence (positive or negative). For instance, a "joy" at $E = 0.8$ and a "sadness" at $E = 0.8$ both indicate a high level of emotional engagement and clarity, albeit with different qualitative experiences. This approach allows the artistic feedback system to map the intensity of the emotional response consistently, using brightness gradients and deformation angles, while the type of emotion determines the specific artistic parameters (e.g., color hue). The color output of the LED array is mapped using the HSV color space. Its hue, saturation, and brightness parameters are set based on the emotion category, and an exponential decay function is applied to adjust the brightness change rate:

$$B(t)=B_0 \cdot e^{-\lambda t}+\Delta B \cdot \left(1-e^{-\lambda t}\right) \tag{11}$$

In formula (11), B_0 is the initial brightness; ΔB is the target brightness offset; λ is the attenuation coefficient; t is the time step, ensuring that the brightness gradient is synchronized with the change in emotional intensity. The thermal actuation response of the shape memory fiber is controlled by current input, and the relationship between the angle ϑ and the driving temperature T is:

$$\theta=k \cdot (T-T_0) \cdot \left(1-e^{-\frac{t}{\tau}}\right) \tag{12}$$

In formula (12), k is the material deformation coefficient; T_0 is the phase change starting temperature; τ is the thermal response time constant, and precise temperature control is achieved by adjusting the current intensity. The synchronization of multimodal feedback is guaranteed by the timestamp alignment algorithm, and the timing offset error τ of LED brightness change and fiber deformation is calculated:

$$\epsilon=\frac{1}{M}\sum_{j=1}^{M}\left|t_{LED,j}\text{-}t_{shape,j}\right| \tag{13}$$

In formula (13), M is the number of sampling points, $t_{LED,j}$ and $t_{shape,j}$ are the feedback triggering times at the j-th moment, and the error is controlled within ±50 ms to maintain perception consistency. Finally, the signal transmission is realized through the conductive fiber network of the knitted base to ensure the stability and real-time performance of the artistic feedback in the garden environment.

System Deployment and Edge Computing Optimization

Based on the lightweight Transformer model, the emotion recognition and art feedback algorithms are deployed on an embedded platform with an integrated knitted substrate, and low-power integration of textile electronics is achieved through conductive fibers and flexible circuits [20,21]. The Qwen-Quantize toolchain is used to quantize the model weights into 8-bit integers, and the absolute mean of the difference between the floating-point value w_f and the quantized value w_q defines the quantization error δ:

$$\delta=\frac{1}{P}\sum_{p=1}^{P}\left|w_f^{(p)}\text{-}w_q^{(p)}\right| \tag{14}$$

In formula (14), P is the total number of parameters. After quantization, the memory usage of the model is reduced to one-fourth of the original floating-point model. In view of the resource constraints of edge computing, a power consumption optimization strategy based on dynamic voltage and frequency adjustment is designed. The relationship between the energy consumption per unit time Z, core frequency f, and supply voltage V_0 is:

$$Z=\alpha C_{eff}{V_0}^2f \tag{15}$$

In formula (15), α is the switching activity factor, and C_{eff} is the effective capacitance; the dynamic power consumption is reduced by lowering the frequency. To reduce signal transmission delay, the resistivity ρ and interconnection length L of the conductive fiber in the knitted structure are optimized, and its parasitic resistance R is calculated according to the following formula:

$$R=\rho\cdot\frac{L}{S} \tag{16}$$

In formula (16), S is the conductive cross-sectional area. By selecting silver-coated polyester fiber and shortening the interconnection path, the single-node transmission delay is controlled. The system realizes modular packaging through the hot-press fusion process of flexible printed circuit boards (PCBs) and knitted substrate. The thermal expansion coefficient and waterproof performance of the packaging material are optimized to ensure mechanical stability and electrical performance consistency under high-span temperature cycles, humidity changes, and potential rain erosion in garden scenes [22,23].

EXPERIMENTAL DESIGN AND MODEL TRAINING

The experimental scene is set up in an open area of a typical urban park, and a representative garden microenvironment is selected to cover natural conditions with different light intensities, temperature gradients, and humidity ranges. The stability of the multimodal data collection accuracy is evaluated by continuously collecting user physiological data and device feedback data within a fixed time period. Emotion recognition is performed by conducting standardized emotion induction tasks in front of the device, and the system recognition results and subjective emotion annotations are recorded simultaneously.

The Art Feedback User Satisfaction Survey measures participants' perceived scores of color gradients, morphological changes, and integration with the natural environment through a combination of on-site experience and questionnaire feedback. The survey uses a 5-point Likert scale (1 = Strongly Disagree, 5 = Strongly Agree) with 15 items across three dimensions (color gradient, dynamic mode, environmental integration). It was administered to 20 participants, and the internal consistency was high (Cronbach's α = 0.87). The system's real-time test records the response delay from data acquisition to LED brightness changes using a high-precision timer, and the resource usage analysis obtains the average current consumption of the model inference phase through the power consumption monitoring module of the embedded platform. The environmental robustness verification is conducted by running the test for 72 hours continuously to record the system stability and data transmission integrity under extreme temperature fluctuations and sudden changes in humidity. This survey was conducted in compliance with the Ethics Committee of Guangxi University of Science and Technology. Participants were informed of the study's purpose and data usage prior to participation, and responses were collected anonymously. No personally identifiable information was stored.

The training of the lightweight Transformer model adopts a phased optimization strategy. The training dataset is a mixture of the DEAP public dataset and a self-built garden scene dataset [24], which contains multimodal features from multi-source sensors. The DEAP data was processed with a 4-second sliding window (50% overlap) to extract valence and arousal labels, which were then mapped to six basic emotions. The dataset was split in a subject-independent manner to prevent data leakage, ensuring that data from any single participant appeared in only one subset. The total number of samples is 12,000 groups, which are divided into a training set, validation set, and test set in the ratio of 8:1:1. The self-built Garden Scene dataset contains 1,200 groups of multimodal data collected from 20 participants (10 males and 10 females, aged 22–45 years) in a typical urban park. Data collection involved performing standardized emotion induction tasks while interacting with a textile installation. The dataset includes simultaneously recorded EMG, electrodermal activity (EDA), speech, and environmental data. Emotion labels were assigned based on a self-reported Likert scale (1–5) and expert annotation of multimodal signal patterns. The model training uses the PyTorch framework, and the training process is divided into two stages: the first stage freezes the underlying parameters of the Transformer and only fine-tunes the cross-modal attention module and classification head to ensure multimodal data alignment; the second stage unfreezes all parameters and accelerates convergence through dynamic precision training. Model compression uses the Qwen-Quantize toolchain to compress weights from 32-bit floating points to 8-bit integers, which improves inference speed and reduces memory usage to meet the real-time requirements of the garden interactive device. After model training, the parameters are initialized, as shown in Table 1.

Table 1. Model Parameter Initialization

Parameter Name	Initialization Value
Learning Rate	1×10^{-4}
Batch Size	64
Optimizer	AdamW (weight_decay = 1×10^{-5})
Loss Function Weight Ratio	Cross Entropy : Knowledge Distillation = 0.7 : 0.3
Transformer Embedding Dimension	128
Number of Attention Heads	4
Network Layers	6
Knowledge Distillation Temperature Coefficient	3
Quantization Bit Width	8-bit Integer
Dynamic Voltage Scaling Frequency Range	80 MHz–240 MHz
Number of Training Epochs / Early Stopping Criteria	50 epochs / Validation loss not decreasing for 5 consecutive rounds
Random Seed	42

PERFORMANCE EVALUATION AND EMOTIONAL-ARTISTIC RESPONSE VERIFICATION OF INTERACTIVE ART INSTALLATIONS IN GARDEN SCENES

Multimodal Data Acquisition Signal Quality Testing

To verify the data stability of the system in complex environments, the signal quality of myoelectric, electrodermal activity, voice, and environmental sensors in different time periods (morning, afternoon, and evening) is evaluated by signal-to-noise ratio (SNR), and dynamic filtering, noise reduction, and time alignment algorithms are applied to optimize data consistency. The evaluation results are shown in Figure 2.

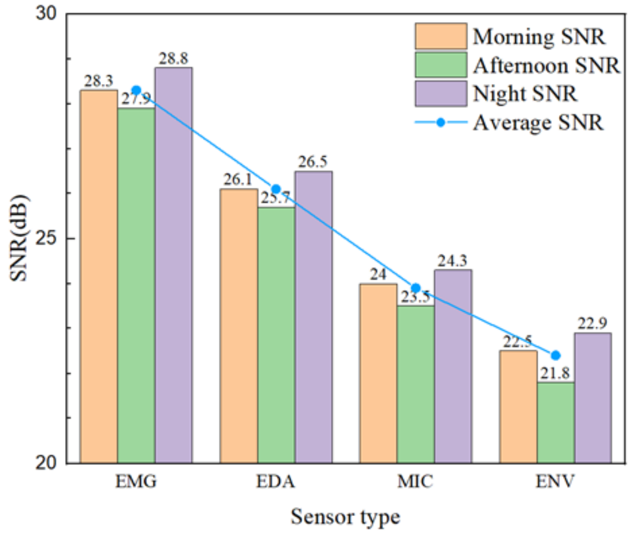

Figure 2. Comparison of Signal Acquisition Quality at Different Time Periods in a Garden Scene

Figure 2 shows the SNR performance of four smart textile sensors in different time periods in a garden scene. The horizontal axis is the sensor type, including EMG, EDA, MIC (microphone), and ENV (environmental sensor); the vertical axis is the signal-to-noise ratio. The SNR for each sensor is calculated as the ratio of the mean signal power to the estimated noise power, which is derived from the variance of the signal during periods of no user interaction. The data show that the EMG sensor maintains a high SNR in all three time periods with little fluctuation, indicating robustness to garden environmental noise; the EDA sensor SNR is second, with an average SNR of 26.1 dB, which drops slightly in the afternoon; the MIC sensor has an average SNR of 23.9 dB, which is relatively low, but stable in the morning and evening; the ENV sensor SNR is lower than other types and drops sharply to 21.8 dB in the afternoon, reflecting its susceptibility to fluctuations in ambient temperature and humidity. The average SNR decreases stepwise from EMG to ENV, revealing differences in data quality among sensors in complex garden scenes and providing a quantitative basis for the reliability of subsequent emotion recognition model input.

Evaluation of Emotion Recognition Effect of Lightweight Transformer Model

The lightweight design of emotion recognition models is the core challenge for smart textiles to achieve real-time interaction in garden scenarios, especially on resource-constrained embedded platforms, where it is necessary to balance computing efficiency and recognition accuracy. The experiment compares the accuracy and F1-score of different models on the DEAP public dataset and the self-built garden dataset. The comparison results are shown in Figure 3.

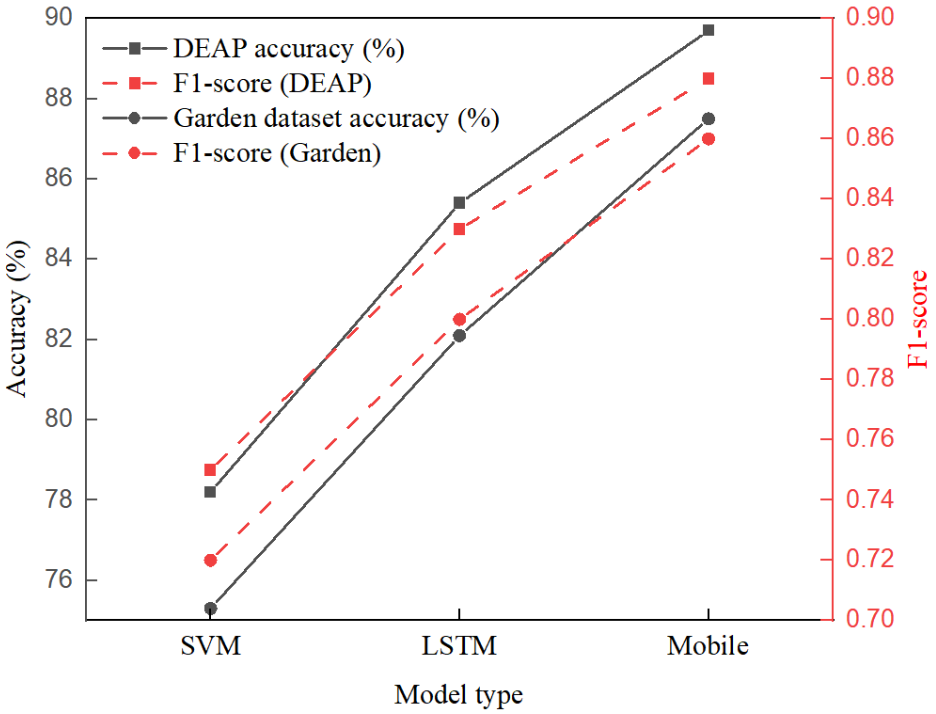

Figure 3. Emotion Recognition Model Performance Comparison

Figure 3 shows the performance differences among three models: SVM, LSTM, and Mobile Transformer, in emotion recognition. The left vertical axis represents accuracy, and the right vertical axis represents F1-score. The data show that Mobile Transformer performs best in both datasets, and its garden accuracy is only 2.2% lower than DEAP, while SVM and LSTM are reduced by 2.9% and 3.3%, respectively, indicating that the lightweight Transformer is more robust to garden environmental noise. The F1-score trend is consistent with accuracy. The Mobile Transformer drops by only 0.02 in the garden data, while the LSTM drops by 0.03, further verifying its stable recognition ability for minority emotions. This performance advantage directly supports the practical value of this method in complex garden scenes.

User Satisfaction Survey of Emotion-Art Feedback Mapping

To verify the effect of the dynamic mapping strategy on improving emotional fit and environmental integration, this section quantifies the impact of art feedback through a user satisfaction survey, focusing on differences in feedback scores across six types of emotions, including joy and calmness. The scoring results are shown in Figure 4.

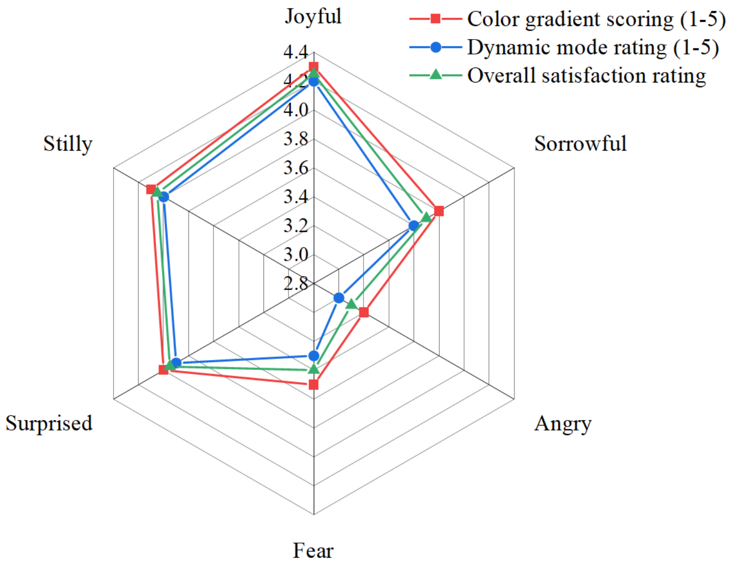

Figure 4. User Satisfaction Survey Results

Figure 4 shows the distribution of color gradient, dynamic mode, and overall satisfaction scores under six emotion categories. To mitigate potential bias in self-reported satisfaction, the survey was conducted in a controlled environment while monitoring users' physiological signals (EMG and EDA). High scores for "joy" and "calmness" correlated strongly with physiological indicators of positive valence and low arousal, objectively validating users' subjective reports.

A strong Pearson correlation ($r = 0.81$, $p < 0.01$) was found between subjective satisfaction scores and objective physiological markers (EMG/EDA), confirming the consistency of user perception. The data show that the three curves of the two positive emotions—joy and calmness—reach more than four points, indicating that the color gradient and dynamic mode effectively convey pleasure, while the curves for the negative emotions of anger and fear shrink, with scores less than 3.5, reflecting that rapid flashing and high-frequency vibration feedback do not match these emotions. The overall satisfaction curve is between the color and dynamic scores. Some emotions, such as surprise, receive extra points due to innovative design. The overall satisfaction score of 3.95 for the emotion "surprise" was second only to the two positive emotion scores, based on qualitative feedback from post-survey interviews. This qualitative insight, combined with the observed physiological startle response (a sharp increase in EDA), confirmed the higher satisfaction scores for this emotion category. These results indicate that users recognize the artistic interactive form. Figure 4 reveals the effectiveness differences of emotional feedback design across emotion categories, providing a basis for subsequent optimization of dynamic mode and enhancement of negative emotion matching.

System Real-Time Performance and Resource Usage Analysis

To verify the system's ability to respond in real time in garden scenarios, the study measures the response delay and resource utilization of the lightweight Transformer on the chip. The response delay here refers to the full-link delay driven by perceptual computing and compares the performance differences between the original model and the compressed model. The comparison results are shown in Figure 5.

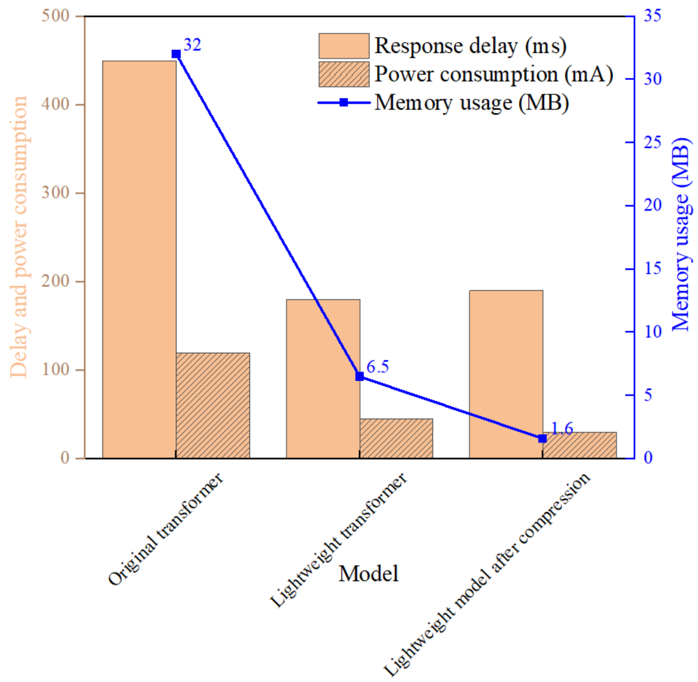

Figure 5. System Performance Comparison

Figure 5 shows the performance comparison among the original Transformer, the lightweight Transformer, and the compressed model in terms of response delay, memory usage, and power consumption. The left vertical axis represents both response delay and power consumption, and the right vertical axis represents memory usage. The key data are as follows: The lightweight Transformer is superior to the original model in response delay and memory usage, which are 180 ms and 6.5 MB, respectively, and power consumption is reduced to 45 mA, indicating that deep separable convolution and the local attention mechanism effectively improve efficiency. The compressed model reduces memory usage to 1.6 MB through 8-bit integer quantization, and power consumption is further reduced to 30 mA, but the response delay slightly increases from 180 ms to 190 ms, reflecting the trade-off in model compression for resource-constrained scenarios. The original model has the worst performance, and the lightweight model is greatly optimized. The compressed model trades a slight increase in latency for extreme compression of memory and power consumption, verifying the practicality of this method in edge computing scenarios in gardens.

System Robustness Testing in Complex Environments

Garden interactive art installations need to be exposed to changing outdoor climates for long periods, facing extreme conditions such as high temperature and sun exposure, low temperature and frost, high humidity and rainfall, and dry, strong winds, which puts higher requirements on the stability of the emotion recognition system. This section simulates the temperature and humidity sudden change scenarios that a typical garden may encounter and evaluates the accuracy fluctuation range of the system under conditions of sudden temperature and humidity changes through a 72-hour continuous operation test. The 72-hour test simulates real-world challenges beyond just temperature and humidity. The environmental chamber was programmed with cyclic profiles of temperature (from −10°C to 45°C) and humidity (from 40% to 90%) to mimic daily fluctuations. To simulate direct sunlight exposure, the textile samples were subjected to 48 hours of UV-A irradiation (1.5 W/m²). Dust and debris were simulated by applying a fine layer of artificial dust and then using a water spray to mimic rainfall, testing the sensor's resistance to clogging and water ingress. The physical integrity of the conductive fibers and flexible circuits was monitored throughout the test, with performance attenuation kept below 10%. This multi-stress simulation demonstrates the system's resilience to key outdoor degradation factors.

The test results are shown in Figure 6.

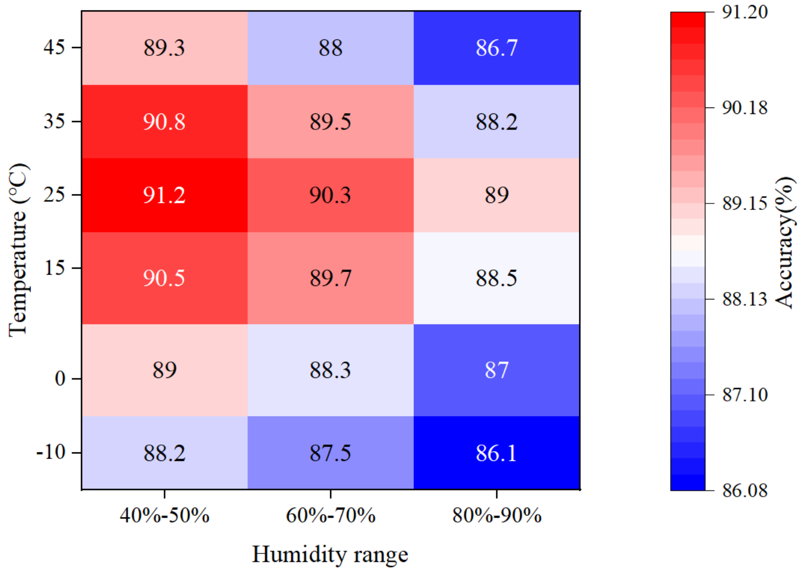

Figure 6. System Robustness in a Simulated Garden Environment with Extreme Temperature and Humidity

Figure 6 shows the trend of emotion recognition accuracy under different temperature and humidity conditions. The data show that the highest accuracy is 91.2% under the combination of 25°C and 40%–50% humidity, while interference is more obvious under extreme environments (−10°C, 80%–90%; 45°C, 80%–90%). The temperature effect is as follows: under 40%–50% humidity, accuracy peaks as the temperature rises from −10°C to 25°C, and drops to 89.3% after rising to 45°C, with an overall fluctuation of less than 3%. The humidity effect is as follows: under 25°C, increasing humidity causes accuracy to drop from 91.2% to 89.0%.

The system performs best in common garden environments (15–35°C, 40%–70% humidity); accuracy in extreme combinations exceeds 85%, proving basic usability. Temperature adaptability analysis shows that the fluctuation in high-temperature environments is slightly greater than in low-temperature environments; accuracy drops by about 2–3% in high-humidity environments, but no mutation errors occur, verifying its robustness to garden noise and extreme conditions.

DISCUSSION

Beyond environmental robustness, practical deployment challenges are addressed. The system is powered by a flexible solar film integrated into the textile, providing sustainable energy in sunlit garden areas. The wearable components are designed for easy cleaning; the conductive fabric is water-resistant, and the sensor nodes are encapsulated in removable, washable silicone sleeves. For durability and maintenance, the system adopts a modular design where the sensing fabric and actuator units are separate. This allows damaged components to be easily repaired or replaced without discarding the entire installation, enhancing long-term sustainability.

Successful validation in experimental garden environments demonstrates the system's potential for broader applications. This technology can be extended to interactive public art installations in urban spaces, museums, or therapeutic gardens, where dynamic emotional feedback can enhance user engagement and well-being. Furthermore, the core framework of emotion-art mapping is adaptable to various smart textile products, paving the way for its industrialization in ambient intelligence and affective computing domains.

CONCLUSION

This study builds an emotion-driven interactive system that is adaptable to garden environments through the coordinated optimization of multimodal data collection, lightweight model design, and dynamic art feedback strategies. The silver-coated fiber sensor integrated on the knitted substrate enables multi-time acquisition of multi-source signals, and the average EMG signal-to-noise ratio reaches 28.3 dB. The lightweight Transformer model compresses the response delay to 190 ms in complex garden scenes through deep separable convolution and the local attention mechanism, verifying the adaptability of model compression to resource-constrained platforms. The emotion-art feedback mapping strategy dynamically matches emotion intensity through gradual changes in LED brightness and the deformation of shape memory fibers. The user satisfaction survey shows that the scores for joy and calmness emotion feedback are 4.25 and 4.05 points, indicating a high degree of fit between artistic expression and emotional characteristics. The study applies the context modeling capability of the lightweight Transformer to smart textiles, constructs a dynamic association mechanism from emotion recognition to artistic expression, and breaks through the real-time bottleneck. However, the accuracy of emotion recognition in simulated garden high-temperature and high-humidity environments still fluctuates, and it is urgent to optimize the sensor anti-interference coating and the adaptive adjustment mechanism of cross-modal attention weights, and further explore the application scenarios of garden art installations with multi-user collaborative interaction and group emotion fusion feedback.

Author Contributions

Conceptualization – Tianlong CHAI; methodology – Tianlong CHAI and Chengcheng SHA; investigation – Chengcheng SHA; writing-original draft preparation – Tianlong CHAI and Chengcheng SHA. All authors have read and agreed to the published version of the manuscript.

Conflicts of Interest

The authors declare no conflict of interest.

Funding

This research was supported by Guangxi Natural Science Foundation under Grant No. 2025JJH160127; Guangxi Eco-Engineering Vocational & Technical College Talent Introduction Research Project No. GXSTKYZX20240603; 2021 Guangxi University of Science and Technology Doctoral Fund Project No.xkb22Z37.

Acknowledgements

Not applicable.

Ethics Approval and Consent to Participate

This survey was conducted in compliance with the Ethics Committee of Guangxi University of Science and Technology. Participants were informed of the study’s purpose and data usage prior to participation, and responses were collected anonymously. No personally identifiable information was stored.

REFERENCES

[1] Manoella G, Joana C, Cabral I. Smart Textile Design: A Systematic Review of Materials and Technologies for Textile Interaction and User Experience Evaluation Methods. Technologies. 2025; 13(6):251. doi: 10.3390/technologies13060251

[2] Oatley G, Choudhury T, Buckman P. Smart Textiles for Improved Quality of Life and Cognitive Assessment. Sensors. 2021; 21(23):8008. doi: 10.3390/s21238008

[3] García-Hernández RA, Luna-García H, Celaya-Padilla JM, García-Hernández A, Reveles-Gómez LC, Flores-Chaires LA, et al. A Systematic Literature Review of Modalities, Trends, and Limitations in Emotion Recognition, Affective Computing, and Sentiment Analysis. Applied Sciences. 2024; 14(16):7165. doi: 10.3390/app14167165

[4] Wu Y, Mi Q, Gao T. A Comprehensive Review of Multimodal Emotion Recognition: Techniques, Challenges, and Future Directions. Biomimetics. 2025; 10(7):418. doi: 10.3390/biomimetics10070418

[5] Beltrán-Escobar M, Alarcón TE, Rumbo-Morales JY, López S, Ortiz-Torres G, Sorcia-Vázquez FDJ. A Review on Resource-Constrained Embedded Vision Systems-Based Tiny Machine Learning for Robotic Applications. Algorithms. 2024; 17(11):476. doi: 10.3390/a17110476

[6] Chen X, Ibrahim Z. A Comprehensive Study of Emotional Responses in AI-Enhanced Interactive Installation Art. Sustainability. 2023; 15(22):15830. doi: 10.3390/su152215830

[7] Jiang M. Movement-Based Interactive Textiles Design for Emotion Regulation. The Design Journal. 2021; 24(3):477-488. doi: 10.1080/14606925.2021.1903678

[8] Dejene BK. Wearable smart textiles for mood regulation: A critical review of emerging technologies and their psychological impacts. Journal of Industrial Textiles. 2025; 55:15280837251314190. doi: 10.1177/15280837251314190

[9] Jiang M, Wang Y, Nanjappan V, Bai Z, Liang HN. E-textiles for emotion interaction: a scoping review of trends and opportunities. Personal and Ubiquitous Computing. 2024; 28(3):549-577. doi: 10.1007/s00779-024-01793-w

[10] Jiang M, Nanjappan V, ten Bhömer M, Liang H-N. On the Use of Movement-Based Interaction with Smart Textiles for Emotion Regulation. Sensors. 2021; 21(3):990. doi: 10.3390/s21030990

[11] Mai ND, Nguyen HT, Chung WY. Deep Learning-Based Wearable Ear-EEG Emotion Recognition System with Superlets-Based Signal-to-Image Conversion Framework. IEEE Sensors Journal. 2024; 24(7):11946-11958. doi: 10.1109/JSEN.2024.3369062

[12] Kumar S. Deep learning based affective computing. Journal of Enterprise Information Management. 2021; 34(5):1551-1575. doi: 10.1108/JEIM-12-2020-0536

[13] Nita S, Bitam S, Heidet M, Mellouk A. A new data augmentation convolutional neural network for human emotion recognition based on ECG signals. Biomedical Signal Processing and Control. 2022; 75:103580. doi: 10.1016/j.bspc.2022.103580

[14] Wu Y, Daoudi M, Amad A. Transformer-Based Self-Supervised Multimodal Representation Learning for Wearable Emotion Recognition. IEEE Transactions on Affective Computing. 2024; 15(1):157-172. doi: 10.1109/TAFFC.2023.3263907

[15] Andayani F, Theng LB, Tsun MT, Chua C. Hybrid LSTM-Transformer Model for Emotion Recognition from Speech Audio Files. IEEE Access. 2022; 10:36018-36027. doi: 10.1109/ACCESS.2022.3163856

[16] Kim H, Rho S, Jeong W. Manufacturing and characterization of conductive threads based on twisting process for applying smartwear. Fashion and Textiles. 2025; 12(1):4. doi: 10.1186/s40691-024-00406-7

[17] Sujiwa A, Maniani BS. The Effect of Inaccurate Electronic Component Values on The Output Frequency Characteristics of Fourth Order Butterworth Type Low-pass Filter Circuits. Faraday: Journal of Fundamental Physics, Research, and Applied Science. 2025; 1(1):1-8. doi: 10.33005/faraday.v1i1.4

[18] Kim ML, Otal EH, Takizawa J, Sinatra NR, Dobson K, Kimura M. All-Organic Electroactive Shape-Changing Knitted Textiles Using Thermoprogrammed Shape-Memory Fibers Spun by 3D Printing. ACS Applied Polymer Materials. 2022; 4(4):2355-2364. doi: 10.1021/acsapm.1c01606

[19] Kim SU, Kim J. Analysis of driving forces of 3D knitted shape memory textile actuators using scale-up finite element method. Fashion and Textiles. 2022; 9(1):38. doi: 10.1186/s40691-022-00307-7

[20] Yang Y, Wei X, Zhang N, Zheng J, Chen X, Wen Q, et al. A non-printed integrated-circuit textile for wireless theranostics. Nature Communications. 2021; 12(1):4876. doi: 10.1038/s41467-021-25075-8

[21] Cleary F, Henshall DC, Balasubramaniam S. On-Body Edge Computing Through E-Textile Programmable Logic Array. Frontiers in Communications and Networks. 2021; 2:688419. doi: 10.3389/frcmn.2021.688419

[22] Kalaš D, Soukup R, Řeboun J, Radouchová M, Rous P, Hamáček A. Novel SMD Component and Module Interconnection and Encapsulation Technique for Textile Substrates Using 3D Printed Polymer Materials. Polymers. 2023; 15(11):2526. doi: 10.3390/polym15112526

[23] Kim H, Choi JG, Oh T, Lee I, Lee H, Jin H, et al. Waterproof and conductive tough fibers for washable e-textile. npj Flexible Electronics. 2025; 9(1):28. doi: 10.1038/s41528-025-00399-3

[24] Khateeb M, Anwar SM, Alnowami M. Multi-Domain Feature Fusion for Emotion Classification Using DEAP Dataset. IEEE Access. 2021; 9:12134-12142. doi: 10.1109/ACCESS.2021.3051281